ISSN 0018-151X, High Temperature, 2020, Vol. 58, No. 6, pp. 835–838. © Pleiades Publishing, Ltd., 2020.
Russian Text © The Author(s), 2020, published in Teplofizika Vysokikh Temperatur, 2020, Vol. 58, No. 6, pp. 895–899.

HEAT AND MASS TRANSFER AND PHYSICAL GASDYNAMICS

Particle Concentration Distribution in a Gas–Droplet Confined Swirling Flow: Euler and Lagrange Approaches

M. A. Pakhomov[a], * and V. I. Terekhov[a], **

[a] *Kutateladze Institute of Thermophysics, Siberian Branch of Russian Academy of Sciences, Novosibirsk, 630090 Russia*

**e-mail: pakhomov@ngs.ru*

***e-mail: terekhov@itp.nsc.ru*

Received March 10, 2020; revised June 1, 2020; accepted June 18, 2020

Abstract—This paper considers the problem of the numerical simulation of the propagation dynamics of a dispersed admixture and heat transfer in a swirling turbulent gas–droplet flow behind a sudden tube expansion. The gas phase is described by a system of three-dimensional Reynolds-Averaged Navier-Stokes equations with taking into account the effect of particles on the transport processes in the carrier phase. The gas-phase turbulence is calculated with the Reynolds stress transport model with allowance for the effect of the dispersed phase. The Euler and Lagrangian descriptions give qualitatively similar results for small droplet sizes of up to $d_1 \le 30$ μm; it is only for the largest particles studied in this paper (with an initial diameter of $d_1 = 100$ μm) did the difference in the calculation results exceed 15%.

DOI: 10.1134/S0018151X20060140

INTRODUCTION

Swirling two-phase flows with solid or liquid particles in the presence of a sudden expansion of a tube or channel are widely used in various practical applications, e.g., to stabilize the combustion process in industrial burners and separators [1, 2]. The interaction between small sprayed droplets and carrier-phase turbulence is a complex and not completely understood process [3]. Sudden tube expansion leads to the appearance of recirculation regions. It has a noticeable effect on the processes of the transfer of momentum and heat and the propagation of the dispersed phase and mainly determines the structure of the separated two-phase flow [4, 5]. The flow swirling also considerably complicates the understanding of the flow pattern and the processes occurring in such flows. Therefore, despite the widespread use of two-phase swirling flows in the presence of particle evaporation in various practical applications, the processes of turbulent transport in such flows remain insufficiently studied.

The goal of the study is to take the first steps in a comparison of the capabilities of the Eulerian and Lagrangian descriptions of two-phase swirling flows and heat transfer in a gas–droplet flow behind a sudden tube expansion in the dynamics of the dispersed phase distribution. This study is a development of recent studies [5, 6], in which the numerical modeling of a two-phase swirling flow behind a sudden expansion of the tube in the presence of droplet evaporation was performed only with the Eulerian approach.

MATHEMATICAL MODEL

The solution uses a system of three-dimensional Reynolds-Averaged Navier-Stokes (RANS) equations that take into account the effect of particles on transport processes in a gas [5, 6]. Figure 1 shows a schematic representation of the flow. The volume concentration of the dispersed phase is low ($\Phi_1 = M_{L1}\rho/\rho_L < 2 \times 10^{-4}$). The particles are sufficiently small ($d_1 < 100$ μm), so the effects of their collisions with each other can be disregarded. Here, M_{L1} is the initial mass concentration of droplets, and ρ and ρ_L are the density of gas and droplets. The basic equations of the model and the method of numerical implementation were considered in more detail in [5, 6], in which the numerical algorithm was tested in comparison with measurement data for two-phase swirling flows.

One of the methods that allows a partial accounting for the complex mixing processes and the anisotropy of the components of the gas-velocity pulsations in separated swirling flows is the use of second moment closure models. The turbulence of the gas phase was calculated with the elliptical model of the Reynolds stress transport [7] with allowance for the effect of the dispersed phase [8].

Two main approaches are used to describe a two-phase flow: Eulerian continuous (so-called two-fluid models) and Lagrangian (trajectory) approaches. Both of these methods have their pros and cons, and they complement each other [9]. In this case, the pluses of one approach are the minuses of the other. In this paper, we present the first results of a comparison of the capabilities of the Eulerian and Lagrangian

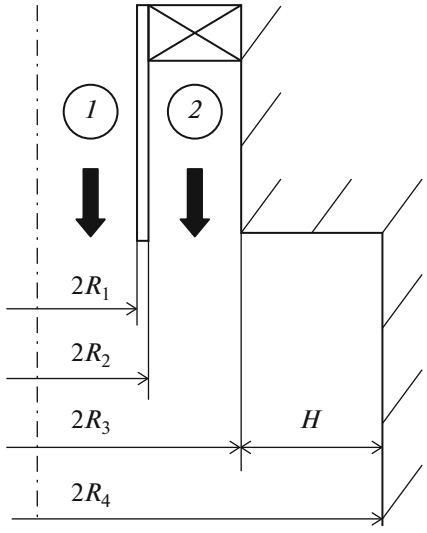

Fig. 1. Diagram of the computational domain: (*1*) two-phase nonswirling gas–droplet flow and (*2*) annular swirling air flow.

methods to describe the dynamics of the dispersed phase in a gas–droplet swirling flow behind a sudden tube expansion.

Eulerian Method

The Eulerian approach is used to describe the flow dynamics and heat and mass transfer in the gas and dispersed phases. The system of equations to model the motion of the dispersed phase in the Eulerian representation was obtained from the kinetic equation for the probability density function of the particle distribution in a turbulent flow [10, 11]. Note that it was initially developed to describe flows with solid particles in the absence of interfacial heat transfer. In this study, this approach is used to describe two-phase flows in the presence of droplet evaporation. The model [10] is used to calculate kinetic stresses and temperature fluctuations and turbulent heat flux in the dispersed phase.

Lagrangian Approach

The gas phase is calculated in the same way as in the Eulerian approach. The action of the following force factors on the particle was taken into account: drag force, gravity, and Saffman forces. The well-known Continuous Random Walk model [12] is used to calculate the dynamics of the dispersed phase with the stochastic Lagrangian approach. This method takes into account the stochastic effect of gas turbulence on particle motion when interphase interaction is a continuous process. This method will be used to calculate the instantaneous (actual) dispersion modeling $\mathbf{U}_{S,i} = \mathbf{U}_i + \mathbf{u}_{S,i}$. Here, $\mathbf{U}_i$ and $\mathbf{u}_{S,i}$ are the components of the averaged gas velocity (determined from the RANS calculation) and the instantaneous gas velocity at the particle location determined from the approach [12]. Random root-mean-square pulsations of the dispersed phase are calculated along a stochastic trajectory, which allows the stochastic nature of the motion of the dispersed phase to be preserved. The expression to calculate the instantaneous value of the gas velocity at the point of the particle location has the form [12]

$$u_{S,i}^m = a_{ij}u_{S,j}^{m-1} + b_{ij}\zeta_j + \mathbf{A}_i\Delta t, \quad \zeta_i \in N(0, 1).$$

Here, the superscript m refers to the current time step, $N(0, 1)$ is a random Gaussian variable having a distribution with a mean value equal to zero and a standard deviation equal to unity, **A** is the vector of the corrected displacement, and Δt is the time step. The expression in [13] is used to calculate the component of the corrected displacement vector:

$$A_{ij} = \frac{1}{1+\mathrm{St}_L}\left[\frac{1}{\rho}\frac{\partial}{\partial x_j}(\rho u_{ij})\right], \quad \mathrm{St}_L = \frac{\tau}{1/7(k/\varepsilon)},$$

where $\tau = \dfrac{\rho_{L2}d_1^2}{3\rho C_D|\mathbf{U}-\mathbf{U}_L|/4}$ is the time of dynamic relaxation of particles. The displacement tensors **a** and diffusion **b** are determined from the following relations given in [12]:

$$a_{ij} = \exp\left(-\frac{\Delta t}{\Omega_L}\right)\delta_{ij}, \quad b_{ik}b_{jk} = (1 - a_{ii}a_{jj})u_{ij},$$

where Ω_L is the turbulent time scale [10, 11]. The transition from trajectory calculations to the distributions of the parameters of the dispersed phase in physical space (e.g., in the calculation of the droplet-concentration field) is performed with space-time averaging of the trajectory data over the control volume of the Eulerian grid used to calculate the gas phase. In this study, 5×10^4 particles were used to obtain a statistically reliable flow pattern.

RESULTS OF NUMERICAL SIMULATION AND THEIR DISCUSSION

A swirling gas—droplet two-phase flow was studied in a downward flow mode behind a sudden tube expansion. The main stream of a mixture of air and water droplets, ethanol, and acetone (*1*, Fig. 1) is fed into the central channel ($2R_1$). A swirling single-phase airflow (*2*) enters the computational domain through an annular channel (R_3-R_2). The geometry of the computational domain is $2R_1 = 20$ mm, $2R_2 = 26$ mm, $2R_3 = 40$ mm, and $2R_4 = 100$ mm, and the step height is $H = 30$ mm. The computational domain length is $X = 1$ m.

The mass-averaged axial velocity of the main air stream is $U_{m1} = 15$ m/s, and its mass flow rate is $G_1 = 5.65$ g/s. The mass-averaged axial velocity and mass flow rate of air in the secondary annular stream are $U_{m2} = 20.7$ m/s and $G_2 = 18$ g/s. The velocity-ratio parameter of coaxial flows in the calculations was a constant value of $m = \rho_2 U_{m2}/\rho_1 U_{m1} = 1.2$, and the swirl

parameter determined by the relation [1, 2] varied in the range of $S = \int_0^{R_3} \rho W_1 U_1 r^2 dr \Big/ \left(R_3 \int_0^{R_3} \rho_1 U_1^2 r dr \right) = 0$–$0.7$. The Reynolds number of the gas phase is $\mathrm{Re} = U_{m1} 2R_1/\nu = 2 \times 10^4$. The wall temperature was constant over the entire length of the computational domain and was equal to $T_W = \mathrm{const} = 373$ K.

The initial, averaged axial velocity of water droplets is $U_{L1} = 12$ m/s. The initial diameter of water droplets is $d_1 = 10$–100 μm, and their mass concentration is $M_{L1} = 0$–0.1. The temperature of air and droplets at the inlet is $T_1 = T_{L1} = T_2 = 293$ K. The calculations were performed at atmospheric pressure. The criterion characterizing the degree of particle involvement in the gas-phase motion is the Stokes number in the averaged motion $\mathrm{Stk} = \tau/\tau_f$, where τ_f is the turbulent time macroscale. For separated two-phase nonswirling flows, the following relation for the relaxation time of the dispersed phase: $\tau_f = 5H/U_{m1} = 0.01$ s is given in [3, 4]. Then, taking into account that $\tau = 0.3$–30 ms for the conditions of the present calculations, $\mathrm{Stk} = 0.03$–2.6. This suggests that the particles can be well involved in the turbulent motion of the gas at $\mathrm{Stk} < 1$ and do not interact with it at $\mathrm{Stk} > 1$ [3, 4].

The effects of the breakup and coalescence of the dispersed phase are not taken into account due to the small number of particles. The volume concentration of the dispersed phase is low ($\Phi_1 = M_{L1}\rho/\rho_L < 2 \times 10^{-4}$). The water droplets are rather small ($d_1 < 100$ μm), so the effects of their collisions with each other can be disregarded, and they have a monodisperse distribution at the inlet. Further, as they move through the tube, the droplet size is variable in all three directions due to heating and evaporation. We understand that disregarding the initial polydispersity of droplets can be important in the analysis of processes occurring in two-phase flows [e.g., 14]. It is assumed in the study that droplets deposited on the tube wall from a two-phase flow instantly evaporate. This assumption is valid for the case of a large temperature difference between the wall and the droplet ($T_W - T_{WL}$) > 40 K [5, 6]. Calculations were performed for nonswirling and swirling two-phase flows with equal mass flow rates of the gas $(G_1 + G_2)_{S \neq 0} = G_{S=0}$ and dispersed $M_{L1,\, S \neq 0} = M_{L1,\, S=0}$ phases.

A change in the inlet particle diameter leads to significant differences in the distribution of the droplet volume concentration along the axis of the swirling two-phase flow. These results are shown in Fig. 2. For small particles ($d_1 = 10$–30 μm), an increase in the concentration of the dispersed phase in the initial sections on the tube axis is observed due to its accumulation in the recirculation zone under the action of a recirculating flow.

The nonuniformity of the turbulent kinetic energy profile of the gas and dispersed phases along the tube radius leads to the turbulent migration of droplets (turbophoresis force) to the tube axis. This also causes the presence of the maximal volume fraction of solid particles on the tube axis in the case of small particles (line *2*, $d_1 = 30$ μm). The most inertial droplets (line *3*, $d_1 = 100$ μm) are characterized by rapid scattering over the tube cross section under the action of centrifugal forces, turbulent diffusion, and turbulent migration.

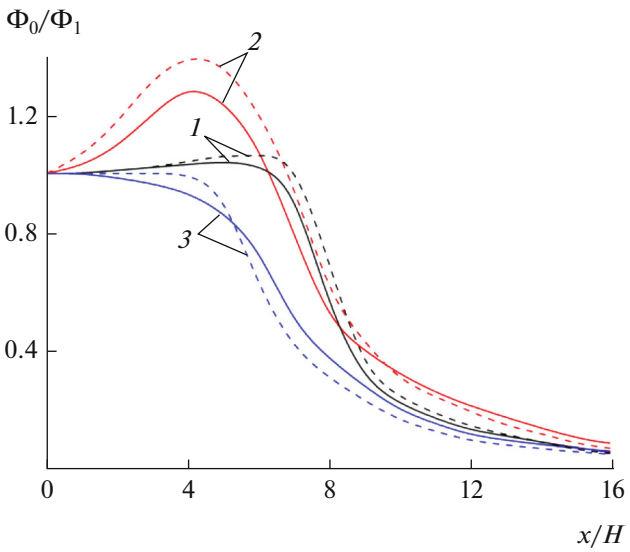

Fig. 2. Distributions of the droplet volume concentration along the tube axis in a swirling, two-phase flow: dashed line, Lagrangian approach; solid curves, Eulerian description; $\mathrm{Re} = 2 \times 10^4$; $M_{L1} = 0.05$; $S = 0.5$; (*1*) $d_1 = 10$; (*2*) 30; and (*3*) 100 μm.

These conclusions are in qualitative agreement with the data from known measurements [15] and large-eddy simulation (LES) [16, 17] for isothermal swirling gas flows with solid particles behind a sudden expansion of the tube. This effect becomes more pronounced with an increase in the initial droplet diameter. It can be noted that the Eulerian and Lagrangian descriptions produce qualitatively similar results for small droplet sizes of up to $d_1 \leq 30$ μm, and only for the largest particles studied here with an initial diameter of $d_1 = 100$ μm does the difference in the calculation results exceed 15%.

In the case of a gas–droplet swirling flow behind a sudden channel expansion, the results of experiments [18] and LES [19] were used for comparisons. Figure 3 shows the calculation results obtained with the Eulerian (*3*) and Lagrangian (*4*) approaches. The swirling two-phase flow of a mixture of air and kerosene droplets was studied in a horizontal flow behind a sudden channel expansion in the presence of particle evaporation of the dispersed phase. The square channel height was 130 mm, and its length was 245 mm. The step height is $H = 50$ mm. The diameter of the nozzle supplying the kerosene was $2R_1 = 5$ mm, and the diameter of the peripheral opening for air supply was $2R_3 = 30$ mm. The

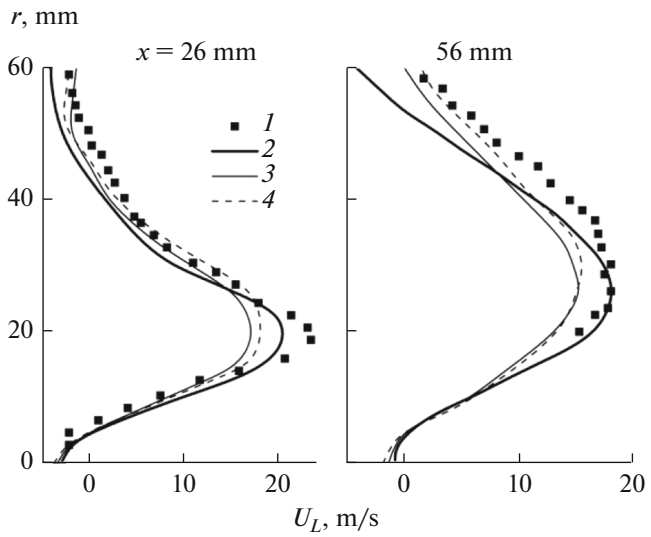

Fig. 3. Distributions of the averaged longitudinal component of the droplet velocity over the channel cross section at $d_1 = 55$ μm, $ML_1 = 0.03$, and $S = 0.7$: (*1*) measurements [18], (*2*) LES calculations [19], (*3*, *4*) calculations in this study with the Eulerian (*3*) and Lagrangian (*4*) approaches.

mass flow rate of the gas was $G_A = 15$ g/s and that of dispersed phase was $G_L = 1$ g/s. The flow swirl number was $S = 0.7$. The average initial air flow velocity was $U_{m1} = 35$ m/s, the Reynolds number was $\mathrm{Re} = U_{m1}2R_3/\nu = 7 \times 10^4$, and the average droplet diameter was $d_1 \approx 55$ μm. The input temperatures of air and kerosene droplets were $T_1 = 463$ K and $T_{L1} = 300$ K. The Stokes number in the averaged motion was $\mathrm{Stk} = 0.6$, and $\tau_f = 5$ ms. This suggests that the droplets are well entrained in the turbulent motion of the gas.

Figure 3 shows the profiles of changes in the averaged longitudinal velocity component of kerosene droplets over the chamber cross section. The comparison results are shown in two sections at a distance from the flow separation position of $x = 26$ ($x/H = 0.52$) and 56 mm ($x/H = 1.12$). The longitudinal component of the droplet velocity is characterized by the presence of a pronounced maximum. In the axial part of the tube, the velocity of the dispersed phase is negative, which indicates the entrainment of droplets in the region of the separated flow. This is true both for these calculations and for measurements and calculations with LES methods [19].

CONCLUSIONS

In general, we note that a qualitative agreement was obtained between the RANS calculations and the measurement data and LES calculations [19]. Eulerian and Lagrangian methods can be used to calculate swirling flows after a sudden tube expansion in the presence of evaporating droplets. Based on the comparison, it is difficult to make an unambiguous conclusion as to which of the two methods produces the best results. It is necessary to perform further studies on the possibilities of application of both approaches to the description of complex two-phase swirling flows in the presence of phase transitions. It is also of great interest to study the effect on the dispersed phase behavior of other factors determining the mixing process, in particular, the channel geometry, the velocity ratio parameter m, the nonisothermality of flows, and others, which will be the subject of further detailed study.

FUNDING

This work was supported by the Russian Science Foundation, project no. 18-19-00161.

REFERENCES

1. Kutateladze, S.S., Volchkov, E.P., and Terekhov, V.I., *Aerodinamika i teplomassoobmen v ogranichennykh vikhrevykh potokakh* (Aerodynamics and Heat and Mass Transfer in Limited Vortex Flows), Novosibirsk: Inst. Teplofiz., Sib. Otd., Akad. Nauk SSSR, 1987.
2. Gupta, A.K., Lilley, D.G., and Syred, N., *Swirl Flows*, Tunbridge Wells: Abacus, 1984.
3. Varaksin, A.Yu., *High Temp.*, 2019, vol. 57, no. 4, p. 555.
4. Fessler, J.R. and Eaton, J.K., *J. Fluid Mech.*, 1999, vol. 314, p. 97.
5. Pakhomov, M.A. and Terekhov, V.I., *Int. J. Thermal Sci.*, 2020, vol. 149, 106180.
6. Pakhomov, M.A. and Terekhov, V.I., *High Temp.*, 2018, vol. 56, no. 3, p. 410.
7. Fadai-Ghotbi, A., Manceau, R., and Boree, J., *Flow, Turbul. Combust.*, 2008, vol. 81, p. 395.
8. Beishuizen, N., Naud, B., and Roekaerts, D., *Flow, Turbul. Combust.*, 2007, vol. 79, p. 321.
9. Nigmatulin, R.I., *Dinamika mnogofaznykh sred* (Dynamics of Multiphase Media), Moscow: Nauka, 1987, vol. 1.
10. Zaichik, L.I., *Phys. Fluids*, 1999, vol. 11, p. 1521.
11. Derevich, I.V., *High Temp.*, 2002, vol. 40, no. 1, p. 78.
12. Moissette, S., Oesterle, B., and Boulet, P., *Int. J. Heat Fluid Flow*, 2001, vol. 22, p. 220.
13. Bocksell, T.L. and Loth, E., *Int. J. Multiphase Flow*, 2006, vol. 32, p. 1234.
14. Tukmakov, A.L. and Tukmakova, N.A., *High Temp.*, 2019, vol. 57, no. 3, p. 398.
15. Sommerfeld, M. and Qiu, H.-H., *Int. J. Heat Fluid Flow*, 1991, vol. 12, p. 20.
16. Apte, S.V., Mahesh, K., Moin, P., and Oefelein, J.C., *Int. J. Multiphase Flow*, 2003, vol. 29, p. 1311.
17. De Souza, F.J., Vasconcelos Salvo, R., and de Moro Martins, D.A., *Sep. Purif. Technol.*, 2012, vol. 94, p. 61.
18. Garcia-Rosa, N., Phenomenes d'allumage d'un foyer de turbomachine en conditions de haute altitude, Ph.D. Thesis, Toulouse: Univ. Toulouse, 2008.
19. Sanjose, M., Senoner, J.M., Jaegle, F., Cuenot, B., Moreau, S., and Poinsot, T., *Int. J. Multiphase Flow*, 2011, vol. 37, p. 514.

Translated by A. Ivanov